

LEGIBILITY NOTICE

A major purpose of the Technical Information Center is to provide the broadest dissemination possible of information contained in DOE's Research and Development Reports to business, industry, the academic community, and federal, state and local governments.

Although a small portion of this report is not reproducible, it is being made available to expedite the availability of information on the research discussed herein.

LCNF-860605--16

Los Alamos National Laboratory is operated by the University of California for the United States Department of Energy under contract W-7405-ENG-36

LA-UR--86-1977

DE86 012379

**TITLE IMPLICIT TWO-FLUID SIMULATION OF ELECTRON TRANSPORT
IN A PLASMA EROSION SWITCH**

RECEIVED BY 100 JUL 07 1986

AUTHOR(S) R. J. Mason, X-1
J. M. Wallace, X-1
K. Lee, X-1

SUBMITTED TO the proceedings of -

The Sixth International Topical Conference on High-Power
Electron and Ion-Beam Research and Technology
Kobe, Japan, June 9-12, 1986

-and-

The Second International Topical Symposium on ICF Research
By High-Power Particle Beams
Nagoaka, Japan, June 16-18, 1986

By acceptance of this article, the publisher recognizes that the U.S. Government retains a nonexclusive, royalty-free license to publish or reproduce
the published form of this contribution, or to allow others to do so, for U.S. Government purposes.

The Los Alamos National Laboratory requests that the publisher identify this article as work performed under the auspices of the U.S. Department of Energy.

Los Alamos Los Alamos National Laboratory
Los Alamos, New Mexico 37545

FORM NO 620-14
G1 NO 2520 6-81

DISTRIBUTION OF THIS DOCUMENT IS UNLIMITED

MASTER

IMPLICIT TWO-FLUID SIMULATION
OF ELECTRON TRANSPORT
IN A PLASMA EROSION OPENING SWITCH

Rodney, J. Mason, Jon M. Wallace and Kenneth Lee

Applied Theoretical Physics Division
Los Alamos National Laboratory
Los Alamos, New Mexico 87545

Abstract

The two-dimensional implicit code ANTHEM is used to model electron transport in Plasma Opening Switches. We look at low density ($\sim 4 \cdot 10^{12} \text{ cm}^{-3}$) switches at initial plasma temperatures as low as 5 eV. Two-fluid modeling (ions and electrons with inertia) and implicit determination of the fields is employed to allow time steps well in excess of the inverse plasma period, and cell sizes much larger than a Debye length — with the avoidance of the finite grid anomalous plasma heating characteristic of particle codes. Features indicative of both erosion and $\mathbf{E} \cdot \mathbf{B}$ plasma drift are manifest in the simulations.

Introduction

In pulse power technology Plasma Erosion Opening Switches are used to minimize prepulse, isotropize the energy delivery, and steepen the time profile of energy delivered to a load. A comprehensive understanding of such switches may prove crucial to the efficient operation of PBFA II light ion diodes.

Early models 1,2 of the switch behavior were based on both experimental and phenomenological considerations. These models described the erosive opening of a gap along the cathode side of the switch, as the E-field of the wave (bringing power down the line) pulled electrons away from the cathode wall. Opening was thought to consist of four phases: 1) For weak currents conduction occurred across a sheath near the cathode with injected ions from the anode, and space charge limited electrons from the cathode. 2) For higher currents the Child-Langmuir electron emission was insufficient, so the gap would widen, providing more effective ion current. This was the "erosion phase". 3) When the magnetic field increased enough in the gap to begin to channel the electrons along the cathode surface, one had the "enhanced erosion phase" and the gap widened more rapidly. 4) Finally, when the magnetic field was large enough to make the

electron gyro-radius smaller than the gap size one had the "magnetic insulation phase". The required 2-D current pattern consistent with this model was evident to some extent in the measurements of Ref. 3.

More recent simulational studies 4,5 suggest a different picture. A gap begins at the cathode near the generator side of the plasma. Electrons then flow in a thin layer on the cathode-facing edge of the plasma, producing the $\mathbf{J} \propto \nabla \times \mathbf{B}$ that cancels the B-field beyond a skin depth inside. Subsequently, $\mathbf{E} \cdot \mathbf{B}$ drift shifts the conduction path inside the plasma over to a diagonal route, which reaches the anode at a progressively closer position to the load. When B has grown large enough to totally insulate the electrons, power is shifted to the load.

These simulational results were obtained with explicit particle-in-cell codes — with their intrinsic limitation to cells no larger than a Debye length, and time steps no larger than a plasma period. To avoid these constraints, to examine the newly pronounced phenomenology, and to calibrate and normalize our own fluidic simulation approach — in anticipation of the modeling of switches at significantly higher density 6 (possibly manifesting classical electron collisionality) — we have applied the implicit ANTHEM simulation code 7,8 to the now canonical low density problem.

The ANTHEM Model

ANTHEM retains the inertial terms in both the ions and the electrons. The electrons can be modeled as either fluids or particles. For the present study the electrons are fluids. The retention of inertia retains a finite electron velocity under the influence of accelerating fields. It also avoids the singularities encountered by conventional hybrid codes near vacuum interfaces. However, because the inertial terms limit conventional explicit treatments to time steps less than a Courant value on the hottest electrons, the fields must be calculated implicitly. The

is accomplished by the Implicit Moment Method 7,8. A set of auxiliary fluid equations is solved self-consistently with Maxwell's Equations for the time-advanced fields. The real fluids are then accelerated in these fields. To avoid excessive numerical diffusion the spatial differencing for the hydrodynamics employs Van Leer corrections. Also, current corrections 8 are applied to assure that quasi-neutrality is maintained, as appropriate, in the calculations.

Special additions for this problem include the implementation of flux transmitting boundary conditions for plasma entering thru the anode side of the switch and absorbing on the cathode, a Child-Langmuir emission module for the cathode surface near the switch plasma, new conduction boundary conditions for the guide walls and its short-circuit load, and a time dependent driven B-field boundary conditions at the generator.

The Low Density Switch Phenomenology

We have modeled the switch configuration considered by Grossman et. al. in 4, but with shorted load condition used by Waisman et. al. in 3. The line between the generator and load is 10 cm in length, and 2.5 cm in width. We use cartesian geometry. Initially, plasma of density $4.0 \times 10^{12} \text{ cm}^{-3}$ flows in a jet of width 5 cm from the top (anode) of the line to its bottom (the cathode) at a speed of $1.8 \times 10^8 \text{ cm/sec}$. At $t = 0$ the B-field starts to grow at $x = 0$, rising linearly to 8 kG in 5 ns. This would correspond to a peak current of 100 kA, if the cathode were a cylinder of 2.5 cm, as in 5. The anode boundary condition is fully transmitting, allowing the penetration of the jet plasma, and absorbing any plasma returning from below. The cathode absorbs all the plasma striking it, but transmits no plasma into the switch region, unless the E-field on cell above the cathode surface exceeds the threshold for Child-Langmuir space charge limited flow. This threshold is usually taken as 300 keV/cm.

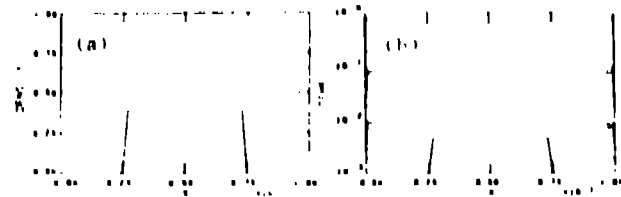


Fig. 1

Figure 1. (a) displays the initial density profile for plasma lying between 2.5 and 7.5 cm in the z -ne. The ions and electrons in the jet are initially at 5 eV, as indicated by Fig. 1 (b). We use a mesh of of 50×50 cells, so $\Delta x = .2$ cm, and $\Delta y = .05$ cm. For this calculation we have set the emission threshold at infinity to test the switch behavior in the absence of Child-Langmuir electrons flowing from the cathode. The B-field is directed into the page.

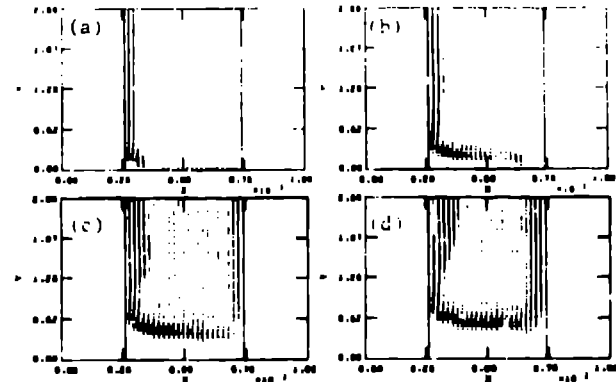


Fig. 2

Figure 2 shows the electron flux patterns at $t = 0.32$, 0.92 , 1.72 and 2.73 ns for frames (a) thru (d), respectively. Figure 3 shows the B-field contours established at these times. At $t = 0.32$ the current runs principally along the generator side of the plasma. Some slight separation from the wall is evident in the lower left-hand corner. By $t = 0.92$ ns separation has proceeded across some 4 cm. of the jet. Electrons flow vertically at the edge of the separation region, then along the lower surface of the jet plasma toward the generator, then vertically within a skin depth (about 0.5 cm in width) of the surface up and along the left face of the jet to the anode. By 1.72 ns there is an

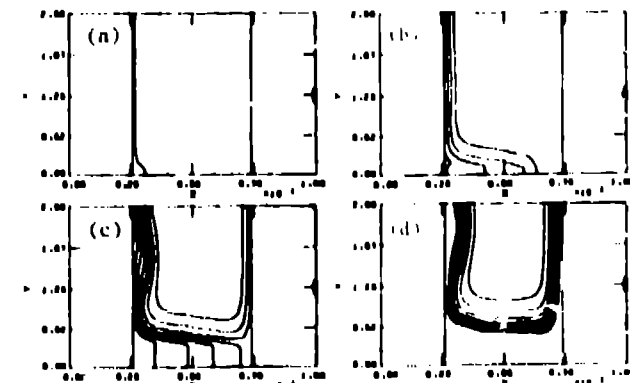


Fig. 3

electron gap along the full lower surface of the jet and the switch is just opening. Other plots show that the ions are also being lifted from the cathode in the erosion process.

The corresponding B-field history in Fig. 3 shows field penetrating the gap, as electrons are removed. The currents along the jet bottom and sides are shielding its interior from the field. Once the gap runs the full plasma length, the field can rush into the void beyond the jet, as current passes to the load. The returning electron flow then runs down the load side of the jet toward the top of the gap, again shielding B on the jet's right side. All this is consistent with the experimental current determinations reported by Weber et. al. in 3.

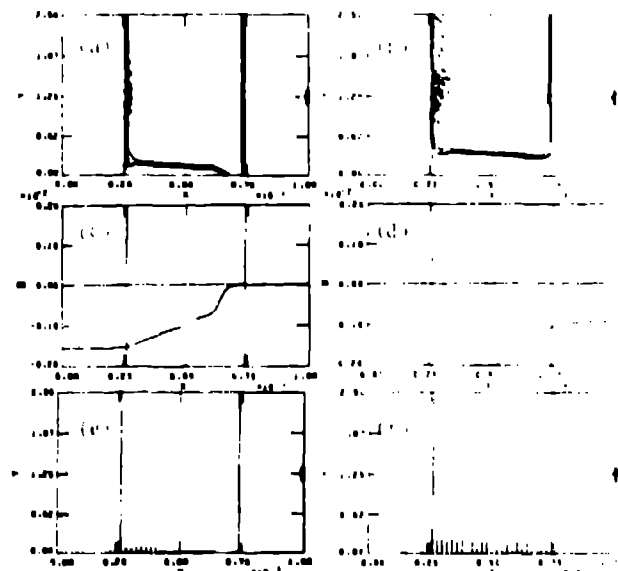


Fig. 4

Figure 4 collects a sampling of output from the code. Frames (a) and (b) show contours of the electron density at $t = 0.92$ and $t = 1.72$, respectively. This could be two-stream instability, since the electron drift speed (here approximately $4\mu\text{m}/\text{ns}$) is considerably higher than the thermal speed (characteristic of 5 eV), and the steep edge gradient may be a significant factor. However, we speculate no further, since more extensive simulation should be obtained first. Frames (c) and (d) plot the B-field in the gap at the two times. The negative scale goes no lower than 2 kG, so that exposition of the later time result is truncated near the generator. The last two frames show respective plots of the E-vector fields. The E-field is largest in the gap, but also significant, as B grows in the left and right voids.

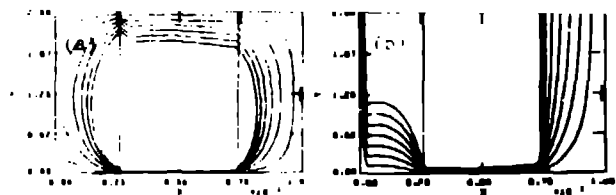


Fig. 5

Final. Figure 5 shows the electrostatic potential and emf-voltage for this run at $t = 1.72$ ns. The potential is used only as a diagnostic in the calculations. Since conductors bound the system above, below and to the right, the potential there is zero. The maximum contour displayed is 50 keV. The voltage contours measure the line integral of \mathbf{E} from the cathode to the anode. Here the maximum displayed line is 200 keV, while the minimum is zero. Clearly, a very large jump exists across the gap, and this should cause Childs-Langmuir emission.

Alternate runs with the space charge emission "on" show a similar behavior at early times -- like that of Figs. 1 and 2 (a) -- but once the Child-Langmuir threshold is surpassed the dynamics changes drastically. Electrons then flow into the plasma from the cathode surface. $\mathbf{E} \cdot \mathbf{B}$ drift ensues, so that the new electrons acquire a significant velocity component along the cathode surface. An electron gap can arise, as in the emission free case, but, with the addition of drifting electrons from below, it acquires a diagonal structure -- running from the lower-left cathode interface upwards in the direction of the load. Switch opening is delayed, by the supply of Child-Langmuir current. As a consequence, electrons running up the generator side of the jet have a longer time to achieve notable $\mathbf{E} \cdot \mathbf{B}$ drift. Traces of such drift are already evident at 1.72 ns in Fig. 1 (d). These features have also been reported in 5. In addition, should the electrons achieve a high temperature from their laminar dynamics, or possibly from instabilities, they may preferentially absorb in the anode. If this occurs leaving a positively charged gap, then B field may penetrate the anode-adjacent plasma, much as it does along the cathode surface, leading to electron drift near the anode, and speedier switching. This has been reported in 3. We have observed this anode drift, when electron entry to the anode was restricted in various tests of the possible boundary condition.

Conclusions

We have demonstrated that two-fluid modeling with implicit fields can be used in the analysis of Plasma Opening Switch dynamics. In application to low density erosion switches, we see many of the features reported from particle code studies. Our Child-Langmuir emission-free calculation matches the current profiles determined experimentally in 3. More fundamentally, we find that the calculated switching behavior is very strongly dependent on our choice of boundary conditions. These may, in fact, be uncertain experimentally, so that additional experimental work into the surface properties at the anode and cathode may be in order. The questions "What is the correct emission threshold?" and "What is the cathode 'saturation' region over which it applies?" remain somewhat open.

Having established the overlap with particle code results that is possible, we are now equipped to explore higher density regions that would be denied to explicit particle codes on account of their inherent limitations. Jet densities as high as 10^{14} cm^{-3} should pose no special challenge. Consequently, the analysis of collisional diffusion of B-fields in such densities should be readily manageable by the ANTHEM Braginskii package 7. Further, the long time exclusion of the jet plasma from the switch by MHD effects should be amenable to the described approach.

Acknowledgements

The authors are grateful to C. Mendel, S. Slutz and P. VanDevender at the Sandia Lab for helpful discussions and encouragement during the course of this work.

References

1. C. W. Mendel, Jr. and S. Goldstein, *J. Appl. Phys.* **48**, (1977), 1604.
2. P. F. Ottinger, S. A. Goldstein, and R. A. Meger, *J. Appl. Phys.* **50**, (1984), 774.
3. B. V. Weber, R. J. Commissa, R. A. Meger, J. M. Neri, W. F. Oliphant and P. F. Ottinger, *Appl. Phys. Lett.* **45**, (1984), 1043.
4. L. M. Warschaw, P. G. Steen, D. E. Parks and A. Wilson, *Appl. Phys. Lett.* **40**, (1982), 1015.
5. J. M. Grossman, P. F. Ottinger, J. M. Neri, D. Mosher and A. T. Drobot, *Bull. Am. Phys. Soc.* **30**, (1985), 1448.
6. Experimental results from C. Mendel et. al., this conference suggest that the PBFA II switch operates at $5 \times 10^{14} \text{ cm}^{-3}$ density.
7. R. J. Mason and C. W. Cranfill, *IEEE Transactions on Plasma Science* **PS-14** (1986), 45.
8. R. J. Mason, "An Electromagnetic Field Algorithm For 2-D Implicit Plasma Simulation", Los Alamos Report LA-UR-86-1391 and submitted to the Jour. Comp. Phys., (May 1986).

DISCLAIMER

This report was prepared as an account of work sponsored by an agency of the United States Government. Neither the United States Government nor any agency thereof, nor any of their employees, makes any warranty, express or implied, or assumes any legal liability or responsibility for the accuracy, completeness, or usefulness of any information, apparatus, product, or process disclosed, or represents that its use would not infringe privately owned rights. Reference herein to any specific commercial product, process, or service by trade name, trademark, manufacturer, or otherwise does not necessarily constitute or imply its endorsement, recommendation, or favoring by the United States Government or any agency thereof. The views and opinions of authors expressed herein do not necessarily state or reflect those of the United States Government or any agency thereof.